

Table IV. Constants for the Redlich-Kister Equation (Eq 1) for Five Isotherms

temp, °C	a	b	c
40.00	1.0229	0.0546	0.0055
60.00	0.9338	0.0687	0.0292
80.00	0.8713	0.0428	-0.0762
100.00	0.8533	0.0428	-0.0664
120.00	0.8248	0.0355	-0.0607

The parameters a and b are concentration dependent, and the mixing rules for binary mixtures are

$$\begin{aligned} a_m &= a_{11}X_1^2 + 2a_{12}X_1X_2 + a_{22}X_2^2 \\ b_m &= b_{11}X_1 + b_{22}X_2 \end{aligned} \quad (8)$$

where a_{12} is given by

$$a_{12} = (1 - k_{12})(a_{11}a_{22})^{1/2}$$

The parameter k_{12} represents the deviation of a_{12} from the classical geometric mean assumption.

For the Redlich-Kwong equation, the values of a_{11} , b_{11} , a_{22} , and b_{22} are evaluated from critical or P - V - T data of the pure components, as recommended by Joffe and Zudkevitch (16, 17). For the PR equation, the temperature dependence of the constant a is given by an expression based on the Pitzer acentric factor (15).

The parameter k_{12} is adjusted by trial and error to produce agreement between the chemical potentials or fugacities in the saturated vapor and liquid phases, a constraint of binary equilibrium. This fitting procedure is applied to an isotherm near the middle of the experimental range (100 °C in this case). k_{12} is assumed to be independent of temperature, pressure, and composition. The calculated interaction parameters for

DME/MeOH are $k_{12} = 0.0252$ for the PR equation and $k_{12} = -0.0065$ for the RK equation.

Tests of the equation of state predictions have been made by comparing experimental and predicted isotherms near the extremes of the experimental range of temperatures. The comparisons are summarized in Figure 7, which shows the fitted isotherm, 100 °C, together with isotherms at 40 and 160 °C. At 40 and 100 °C the predictions of the PR and RK equations are indistinguishable. At 160 °C, neither equation agrees well with experiment over the entire range of pressures; however, the PR equation is marginally better.

Literature Cited

- (1) Tsang, C. Y.; Streett, W. B. *J. Chem. Eng. Data* 1981, 26, 155.
- (2) Chang, C. D.; Silvestri, A. J. *J. Catal.* 1977, 47, 249.
- (3) Harney, B. M.; Mills, A. G. *Hydrocarbon Process.* 1980, 59, 67.
- (4) Van Ness, H. C.; Byer, S. M.; Gibbs, R. E. *AIChE J.* 1973, 19, 236.
- (5) Byer, S. M.; Gibbs, R. E.; Van Ness, H. C. *AIChE J.* 1973, 19, 245.
- (6) Abbott, M. M.; Van Ness, H. C. *AIChE J.* 1975, 21, 62.
- (7) Barker, J. A. *Aust. J. Chem.* 1953, 6, 207.
- (8) Calado, J. C. G. *Técnica* 1972, 34, 237.
- (9) Tsionopoulos, C. *AIChE J.* 1974, 20, 263.
- (10) Chueh, P. L.; Prausnitz, J. M. *AIChE J.* 1967, 13, 896.
- (11) Kell, G. S.; McLaren, G. E. J. *J. Chem. Phys.* 1969, 51, 4345.
- (12) Zubarev, V. N.; Prusakov, P. G.; Sergeeva, L. V., data obtained from IUPAC Thermodynamic Table Project Center, Imperial College of Science, London, 1980.
- (13) Cardoso, E.; Bruno, A. *J. Chem. Phys.* 1923, 20, 347.
- (14) Redlich, O.; Kwong, J. W. S. *Chem. Rev.* 1949, 44, 233.
- (15) Peng, D. Y.; Robinson, D. B. *Ind. Eng. Chem. Fundam.* 1976, 15, 159.
- (16) Joffe, J.; Zudkevitch, D. *AIChE J.* 1970, 16, 112.
- (17) Joffe, J.; Schroeder, G. M.; Zudkevitch, D. *AIChE J.* 1970, 16, 496.

Received for review July 24, 1981. Accepted February 8, 1982. Acknowledgment is made to the donors of the Petroleum Research Fund, administered by the American Chemical Society, for partial support of this work. This work was also supported, in part, by a grant from the Mobil Research and Development Corp. and by grants CPE 78-23537 and 79-09166 from the National Science Foundation.

Partial Miscibility Behavior of the Ternary Systems Methane-Propane-*n*-Octane, Methane-*n*-Butane-*n*-Octane, and Methane-Carbon Dioxide-*n*-Octane

John D. Hotovy, James P. Kohn,* and Kraemer D. Luks†

Department of Chemical Engineering, University of Notre Dame, Notre Dame, Indiana 46556

The phase behavior of three ternary systems (methane-propane-*n*-octane, methane-*n*-butane-*n*-octane, methane-carbon dioxide-*n*-octane) was studied in their regions of L_1-L_2-V immiscibility. Liquid-phase composition and molar volume data for both liquid phases are presented as a function of temperature and pressure in the three-phase region. The boundaries of the three-phase regions, loci of K points ($L_1-L_2 = V$), LCST points ($L_1 = L_2-V$), and Q points ($S-L_1-L_2-V$) are detailed. A detailed study of the immiscibility behavior of the binary system carbon dioxide-*n*-octane is also presented.

Introduction

We have undertaken an extensive study of liquid-liquid-vapor (L_1-L_2-V) phenomena in liquefied natural gas (LNG) systems.

*Recent address: Department of Chemical Engineering, University of Tulsa, Tulsa, Ok 74104.

In an earlier paper (1), we reported the L_1-L_2-V immiscibility region, including its K-point ($L_1-L_2 = V$), LCST ($L_1 = L_2-V$), and Q-point ($S-L_1-L_2-V$) boundaries, for the ternary system methane-ethane-*n*-octane. This system does not exhibit immiscibility in any of its binary pairs. Although immiscibility has been reported in binary systems of methane-*n*-hexane (2) and methane-*n*-heptane (3), solutes such as *n*-octane and higher normal paraffins crystallize as temperature decreases before any immiscibility occurs (4). On the other hand, with ethane as solvent, solutes beginning with *n*-C₁₀ and higher *n*-paraffins demonstrate L_1-L_2-V behavior (5-7). Apparently, the addition of modest amounts of ethane to methane creates a solvent mixture capable of exhibiting immiscibility with *n*-octane.

In this present paper, we present results on three new ternary systems which exhibit immiscibility due to the addition of a heavier solvent species to the binary system methane-*n*-octane. The additives for the three new ternary systems are propane, *n*-butane, and carbon dioxide, respectively. With propane, only very long-chain hydrocarbons (*n*-C₃₇ and higher *n*-paraffins) demonstrate binary L_1-L_2-V behavior (6). Carbon

Table I. Raw Data of the *n*-Octane-Lean Phase (L_1) for the Methane-Propane-*n*-Octane System

type of data	temp, press.,		mole fraction of propane	mole fraction of <i>n</i> -octane	molar vol, mL/(g mol)
	K	atm			
K ($L_1-L_2=V$)	213.07	67.7	0.078	0.0083	73.7
	210.65	65.1	0.065	0.0048	75.4
	206.83	60.9	0.050	0.0039	78.3
	205.72	59.5	0.044	0.0036	80.3
	204.72	58.7	0.039	0.0026	83.8
	201.92	56.0	0.028	0.0016	88.4
Q ($S-L_1-L_2-V$)	199.70	53.8	0.027	0.0022	77.8
	199.61	53.5	0.029	0.0026	73.7
	199.05	52.3	0.039	0.0051	68.6
	198.90	51.7	0.043	0.0061	66.5
	198.58	51.1	0.047	0.0073	64.8
	198.49	50.8	0.051	0.0091	64.3
	198.03	49.5	0.061	0.0125	61.1
	197.90	49.8	0.063	0.0134	61.8
	197.86	49.1	0.066	0.0146	61.3
	197.61	49.0	0.069	0.0158	60.8
	197.31	48.3	0.076	0.0190	59.7
	197.25	47.8	0.079	0.0212	59.1
	196.81	47.0	0.107	0.0385	58.9
LCST ($L_1=L_2=V$)	211.06	64.8	0.123	0.0316	62.9
	210.53	64.1	0.120	0.0319	61.4
	205.99	58.4	0.134	0.0519	61.4
	204.93	57.1	0.130	0.0503	61.4
	203.96	55.8	0.128	0.0493	60.6
	201.11	52.3	0.131	0.0619	60.8
	199.71	50.4	0.126	0.0594	60.1
	197.82	48.2	0.121	0.0567	59.9
L_1-L_2-V	209.54	63.5	0.075	0.0083	59.9
	208.79	61.0	0.111	0.0283	61.1
	207.79	61.7	0.069	0.0073	64.5
	207.04	59.0	0.106	0.0268	61.5
	205.31	56.9	0.101	0.0257	62.0
	204.00	57.6	0.050	0.0057	72.5
	204.00	57.3	0.055	0.0070	68.4
	204.00	57.2	0.059	0.0071	66.3
	204.00	56.0	0.087	0.0022	61.4
	203.47	55.3	0.088	0.0024	60.0
	203.20	56.2	0.059	0.0090	63.1
	203.20	56.8	0.049	0.0550	70.8
	202.74	56.5	0.039	0.0045	76.4
	202.23	55.2	0.052	0.0072	64.2
	202.00	54.9	0.054	0.0081	67.2
	202.00	54.7	0.059	0.0097	65.8
	202.00	54.3	0.066	0.0111	64.6
	202.00	54.0	0.073	0.0129	62.9
	202.00	53.3	0.089	0.0243	60.5
	202.00	55.2	0.049	0.0070	69.3
	201.57	54.6	0.041	0.0050	66.7
	201.04	54.2	0.048	0.0069	68.2
	200.70	51.8	0.090	0.0247	59.5
	200.09	54.1	0.028	0.0023	76.7
	200.10	53.6	0.038	0.0044	71.1
	200.12	53.2	0.043	0.0054	68.6
	200.11	53.1	0.046	0.0062	67.5
	200.10	52.9	0.049	0.0770	67.1
	200.10	52.2	0.060	0.0114	63.5
	200.10	51.9	0.066	0.0134	63.1
	200.10	51.4	0.076	0.0169	61.4
	200.09	51.0	0.092	0.0255	60.0
	200.03	53.2	0.064	0.0134	63.2
	199.99	53.1	0.044	0.0065	65.1
	199.94	53.3	0.039	0.0052	67.6
	199.03	50.1	0.084	0.0226	59.3
	198.42	49.3	0.085	0.0230	59.3
	198.40	49.7	0.074	0.0209	60.4
	198.00	49.3	0.065	0.0143	61.5
	198.00	48.9	0.079	0.0197	60.6
	198.00	48.4	0.094	0.0285	60.6

dioxide will exhibit immiscibility with *n*-octane (7). (Immiscibility of CO_2 with *n*-paraffins has been reported (8) and varies from

Table II. Raw Data of the *n*-Octane-Rich Phase (L_1) for the Methane-Propane-*n*-Octane System

type of data	temp, press.,		mole fraction of propane	mole fraction of <i>n</i> -octane	molar vol, mL/(g mol)
	K	atm			
K ($L_1-L_2=V$)	212.96	67.6	0.150	0.052	62.8
	210.40	64.2	0.165	0.092	64.5
	208.91	63.2	0.164	0.107	68.1
	205.54	59.5	0.160	0.153	69.4
	202.86	56.8	0.144	0.194	71.1
	201.50	55.7	0.136	0.205	70.1
	200.98	55.2	0.132	0.217	71.6
Q ($S-L_1-L_2-V$)	199.17	52.5	0.129	0.218	71.6
	199.05	52.1	0.130	0.212	70.5
	198.71	51.5	0.133	0.198	69.3
	198.69	51.4	0.135	0.197	69.9
	198.35	50.3	0.135	0.180	66.5
	197.69	48.7	0.142	0.146	65.0
	197.06	47.4	0.141	0.091	61.2
L_1-L_2-V	208.35	61.5	0.141	0.055	60.8
	207.04	59.9	0.137	0.053	61.0
	206.52	59.2	0.135	0.052	61.0
	206.82	59.8	0.154	0.085	62.5
	205.30	57.6	0.141	0.068	60.2
	204.47	58.6	0.147	0.151	63.6
	204.09	58.0	0.151	0.157	66.6
	204.00	56.8	0.154	0.132	64.1
	204.00	56.7	0.152	0.126	63.3
	204.00	56.5	0.151	0.116	62.3
	205.93	54.5	0.147	0.091	61.4
	202.88	54.4	0.135	0.064	60.2
	202.35	55.9	0.134	0.1690	63.6
	202.00	56.0	0.141	0.2000	70.4
	202.00	55.9	0.139	0.1940	68.6
	202.00	55.7	0.139	0.1890	68.1
	202.00	54.5	0.152	0.1490	65.5
	202.00	54.0	0.151	0.1300	63.5
	202.00	53.7	0.148	0.1140	62.4
	201.65	52.8	0.144	0.0890	61.4
	201.65	55.8	0.132	0.1980	68.0
	200.48	53.9	0.133	0.1980	68.9
	200.48	54.0	0.133	0.2000	68.9
	200.30	51.0	0.141	0.0870	61.2
	200.08	53.8	0.130	0.2180	71.5
	200.08	53.8	0.130	0.2160	71.2
	200.07	53.7	0.131	0.2130	70.7
	200.10	53.3	0.135	0.2020	70.0
	200.10	53.2	0.136	0.1960	69.0
	200.10	52.8	0.138	0.1850	68.0
	200.07	52.3	0.148	0.1620	66.0
	200.07	52.1	0.149	0.1520	65.2
	200.07	51.9	0.149	0.1420	64.4
	200.10	51.4	0.147	0.1260	62.9
	200.10	51.0	0.141	0.1030	60.3
	199.37	50.9	0.143	0.1480	65.4
	199.33	49.9	0.138	0.0850	61.2
	199.25	49.7	0.129	0.0700	59.8
	198.00	49.0	0.144	0.145	64.7
	198.00	48.7	0.146	0.126	63.6
	198.00	48.3	0.142	0.102	62.5
	198.14	48.1	0.135	0.083	60.8

n-heptane (9) up to *n*-eicosane (10, 11). Data presented herein include liquid-phase composition and molar volume for both liquid phases in the L_1-L_2-V regions at various pressures and temperatures, as well as data on the bounding loci of the L_1-L_2-V region. These loci are K points, LCST, and Q points as in the earlier study of methane-ethane-*n*-octane (1). The extent of the L_1-L_2-V regions in these three new ternary systems will be compared to that of methane-ethane-*n*-octane in pressure-temperature space. As before, the solid phase when present will be *n*-octane.

The immiscibility region for the binary system CO_2 -*n*-octane will also be mapped out in detail. Immiscibility occurs here in

Table III. Raw Data of the *n*-Octane-Lean Phase (L_2) for the Methane-*n*-Butane-*n*-Octane System

type of data	mole fraction of <i>n</i> -butane mole fraction of <i>n</i> -octane molar vol, mL/(g mol)				
	temp, K	press., atm	<i>n</i> -butane	<i>n</i> -octane	mL/(g mol)
K ($L_1-L_2 = V$)	206.44	63.2	0.045	0.0046	72.9
	204.28	60.3	0.029	0.0025	79.5
	203.28	59.3	0.023	0.0029	82.6
	202.09	57.4	0.020	0.0019	86.3
	201.77	57.2	0.022	0.0230	83.5
	197.96	53.0	0.012	0.0017	90.5
Q ($S-L_1-L_2-V$)	197.57	52.6	0.012	0.0017	87.0
	197.45	52.3	0.017	0.0031	72.8
	197.02	51.5	0.022	0.0039	70.6
	196.78	50.9	0.025	0.0046	68.9
	196.25	49.9	0.031	0.0060	67.6
	196.20	50.0	0.029	0.0059	65.9
	195.84	49.2	0.037	0.0075	67.3
	195.65	49.0	0.036	0.0075	64.4
	195.59	48.9	0.040	0.0081	64.5
	195.39	48.6	0.042	0.0089	62.8
	195.07	47.9	0.047	0.1030	62.4
	194.85	47.5	0.052	0.0097	62.5
	194.07	46.1	0.061	0.0170	59.4
	193.83	45.7	0.068	0.0202	59.1
	193.49	45.1	0.088	0.0314	59.7
LCST ($L_1 = L_2 = V$)	204.61	60.2	0.086	0.0186	60.5
	202.47	57.2	0.102	0.0278	60.5
	197.16	49.8	0.106	0.0383	59.5
	195.64	47.8	0.108	0.0425	60.9
	193.48	45.0	0.098	0.0384	60.0
L_1-L_2-V	206.00	62.5	0.053	0.0071	63.9
	204.92	61.0	0.048	0.0059	69.5
	204.00	59.6	0.063	0.0077	64.4
	204.00	59.4	0.070	0.0141	62.9
	206.00	62.5	0.053	0.0071	63.9
	204.92	61.0	0.048	0.0059	69.5
	204.00	59.6	0.063	0.0077	64.4
	204.00	59.4	0.070	0.0141	62.9
	202.00	57.3	0.035	0.0048	70.1
	201.95	57.0	0.026	0.0050	76.3
	202.00	57.0	0.044	0.0072	64.6
	202.00	56.8	0.035	0.0082	65.3
	202.00	56.7	0.073	0.0126	61.6
	202.00	56.5	0.072	0.0145	62.0
	201.15	56.3	0.036	0.0097	70.3
	200.00	55.2	0.022	0.0031	77.3
	200.00	55.0	0.023	0.0037	73.0
	200.00	54.9	0.028	0.0041	70.4
	200.00	54.8	0.030	0.0047	68.3
	200.00	54.6	0.036	0.0055	67.6
	200.01	54.4	0.040	0.0064	65.8
	200.00	53.8	0.087	0.0229	60.0
	198.00	52.6	0.023	0.0042	71.8
	197.99	52.3	0.028	0.0054	69.4
	198.00	52.1	0.033	0.0063	66.8
	198.00	52.0	0.036	0.0063	65.6
	198.00	51.9	0.039	0.0072	64.3
	198.00	51.2	0.069	0.0161	61.0
	196.00	49.3	0.035	0.0075	63.9
	196.00	49.1	0.042	0.0091	62.9
	196.00	48.5	0.075	0.0203	59.2

a CO₂-rich system, while immiscibility in the system methane-carbon dioxide-*n*-octane is in the methane-rich portion of phase space. Consequently, these two regions of immiscibility are not connected.

Experimental Section

The apparatus used in this study was the same as that used by Kohn and co-workers in other cryogenic studies (3). The procedures for studying L_1-L_2-V phenomena and the associated boundaries of the L_1-L_2-V region are detailed elsewhere (1, 12). Briefly, all experiments were carried out in visual glass cells, using stoichiometry and volumetric measurements to

Table IV. Raw Data of the *n*-Octane-Rich Phase (L_1) for the Methane-*n*-Butane-*n*-Octane System

type of data	mole fraction of <i>n</i> -butane mole fraction of <i>n</i> -octane molar vol, mL/(g mol)				
	temp, K	press., atm	<i>n</i> -butane	<i>n</i> -octane	mL/(g mol)
K ($L_1-L_2 = V$)	206.39	63.0	0.113	0.032	62.6
	205.63	62.2	0.127	0.039	61.1
	203.90	59.9	0.145	0.063	59.4
	203.62	59.5	0.149	0.068	60.3
	203.41	59.3	0.153	0.072	62.5
	201.45	56.9	0.159	0.107	64.1
	200.20	55.6	0.156	0.131	66.0
	198.93	54.1	0.149	0.161	68.4
Q ($S-L_1-L_2-V$)	196.31	50.2	0.145	0.162	68.3
	196.09	49.8	0.147	0.158	68.1
	195.07	48.1	0.146	0.128	65.6
	194.85	47.6	0.148	0.123	65.5
	194.10	46.3	0.142	0.098	63.2
	193.91	46.0	0.144	0.097	61.7
L_1-L_2-V	204.00	59.6	0.109	0.030	59.9
	204.00	59.5	0.114	0.033	60.1
	203.79	59.1	0.110	0.030	60.2
	203.00	58.6	0.150	0.068	61.0
	202.00	57.1	0.151	0.071	62.1
	202.00	57.0	0.146	0.067	61.6
	202.00	56.6	0.130	0.049	60.2
	200.00	55.2	0.152	0.127	64.4
	200.00	55.2	0.152	0.128	64.7
	200.00	54.6	0.151	0.104	63.2
	200.00	54.6	0.153	0.103	63.8
	200.00	54.0	0.137	0.064	61.3
	200.00	53.9	0.139	0.063	61.5
	200.00	53.7	0.121	0.045	60.3
	198.00	52.7	0.146	0.161	67.7
	198.00	52.6	0.147	0.160	68.2
	198.00	52.3	0.150	0.130	65.2
	198.00	52.2	0.153	0.127	66.0
	198.00	51.7	0.146	0.105	63.0
	198.00	51.6	0.150	0.101	63.6
	198.00	51.6	0.151	0.100	63.8
	198.00	51.2	0.137	0.067	61.0
	198.00	51.1	0.131	0.060	60.2
	196.00	49.4	0.149	0.129	65.4
	196.00	49.3	0.149	0.123	64.9
	196.00	48.9	0.148	0.103	63.5
	196.00	48.8	0.147	0.098	63.2
	196.00	48.5	0.127	0.060	59.7
	196.00	48.4	0.122	0.055	60.4
	195.00	47.1	0.118	0.054	59.4

compute liquid-phase compositions and molar volumes in L_1 and L_2 . Temperatures were measured with a platinum resistance thermometer and are estimated to be accurate to ± 0.03 K of the 1968 IPTS scale. Pressure measurements were taken with a Heise Bourdon tube gauge, accurate to at least ± 0.07 atm. The gauge was occasionally compared to a dead-weight piston gauge. Liquid-phase volumes could be read to ± 0.02 mL, which translated into a maximum of $\pm 1.6\%$ in molar volumes. *n*-Octane compositions in the L_1 phase are reliable to at least $\pm 2\%$; *n*-octane compositions in the L_2 phase are reliable to at least $\pm 8\%$. Compositions of propane, *n*-butane, and carbon dioxide are reliable to $\pm 3.5\%$.

The methane used in this study was Linde "Ultra Pure" grade stated to be 99.97 mol % pure; it was used without further purification. At 185.06 K, the methane exhibited a difference between dew-point and bubble-point pressures of less than 0.20 atm.

The *n*-octane was a Humphrey-Wilkinson Chemical Co. product with a stated purity of 99 mol %. The measured air-saturated freezing point agreed to within 0.2 K of current literature values. The *n*-octane was used without further purification.

The propane and the *n*-butane were Linde "Instrument

Table V. Raw Data of the *n*-Octane-Lean Phase (L_2) for the Methane-Carbon Dioxide-*n*-Octane System

type of data	temp., press., K	atm	mole fraction of carbon dioxide	mole fraction of <i>n</i> -octane	molar vol., mL/(g mol)
			0.251	0.0146	67.5
K ($L_1-L_2 = V$)	219.73	69.7	0.251	0.0146	67.5
	217.32	67.0	0.221	0.0094	73.1
	214.71	64.3	0.200	0.0075	74.9
	212.20	62.0	0.179	0.0055	78.3
	211.03	60.9	0.163	0.0040	82.7
	207.61	57.9	0.146	0.0044	79.9
	204.83	55.7	0.119	0.0029	84.7
	204.04	55.0	0.107	0.0039	89.8
Q ($S-L_1-L_2-V$)	202.40	53.7	0.110	0.0045	77.0
	202.27	53.2	0.114	0.0056	73.3
	202.16	52.6	0.123	0.0070	69.4
	202.14	52.5	0.131	0.0072	68.0
	201.98	51.5	0.146	0.0097	64.3
	201.43	48.9	0.205	0.0223	56.8
	201.41	48.7	0.199	0.0297	58.0
	201.38	48.0	0.227	0.0302	55.9
	201.08	47.1	0.253	0.0515	54.5
LCST ($L_1 = L_2-V$)	213.54	61.4	0.298	0.0800	58.1
	218.21	67.3	0.291	0.0704	58.2
	215.33	63.7	0.301	0.0646	57.5
	211.73	59.2	0.290	0.0719	58.5
	210.14	57.5	0.289	0.0750	57.0
	206.97	53.5	0.278	0.0712	56.1
	206.29	52.8	0.280	0.0848	56.5
	205.69	51.9	0.275	0.0833	56.3
	203.84	50.1	0.273	0.0817	55.8
L_1-L_2-V	216.00	65.5	0.237	0.0133	66.3
	216.00	65.3	0.247	0.0198	62.3
	214.00	63.2	0.234	0.0157	64.1
	214.00	62.8	0.246	0.0218	61.6
	214.00	62.5	0.256	0.0274	60.6
	212.00	60.8	0.230	0.0173	62.3
	212.00	60.5	0.241	0.0209	61.2
	212.00	60.1	0.255	0.0293	60.9
	212.00	59.9	0.264	0.0335	59.5
	210.00	58.7	0.228	0.0183	61.0
	210.00	58.5	0.231	0.0201	59.3
	210.00	57.5	0.259	0.0355	59.0
	208.00	56.7	0.208	0.0151	61.6
	208.00	56.1	0.223	0.0199	59.6
	208.00	55.9	0.231	0.0232	59.2
	208.00	55.4	0.244	0.0294	57.8
	208.00	55.3	0.249	0.0309	57.6
	208.00	55.2	0.259	0.0363	56.5
	208.00	54.9	0.272	0.0517	56.0
	206.00	55.9	0.154	0.0093	69.3
	206.00	54.5	0.205	0.0167	60.2
	206.00	54.2	0.212	0.0182	59.4
	206.00	53.6	0.226	0.0239	57.9
	206.00	53.4	0.234	0.0265	57.5
	206.00	52.8	0.252	0.0374	56.7
	206.00	52.7	0.261	0.0399	55.3
	204.00	54.9	0.115	0.0037	81.7
	204.00	54.6	0.130	0.0063	75.4
	204.00	54.5	0.134	0.0062	71.6
	204.00	54.2	0.142	0.0080	69.6
	204.00	53.3	0.160	0.0111	65.2
	204.00	52.0	0.203	0.0185	58.8
	204.00	51.6	0.214	0.0214	57.7
	204.00	51.4	0.216	0.0231	57.4
	204.00	51.2	0.224	0.0253	57.0
	204.00	51.0	0.235	0.0307	56.3
	204.00	50.6	0.251	0.0395	55.1
	204.00	50.4	0.255	0.0445	55.8
	204.00	50.2	0.265	0.0555	54.9
	202.00	51.6	0.145	0.0099	65.0
	202.00	49.6	0.205	0.0212	57.2
	202.00	49.3	0.212	0.0239	56.4
	202.00	48.8	0.226	0.0301	56.3
	202.00	48.1	0.253	0.0472	54.7
	202.00	47.9	0.255	0.0521	55.0

Table VI. Raw Data of the *n*-Octane-Rich Phase (L_1) for the Methane-Carbon Dioxide-*n*-Octane System

type of data	temp., K	press., atm	mole fraction of carbon dioxide	mole fraction of <i>n</i> -octane	molar vol., mL/(g mol)
			0.322	0.0718	58.5
K ($L_1-L_2 = V$)	220.78	70.7	0.322	0.0718	58.5
	220.08	70.7	0.323	0.0828	59.0
	218.99	68.8	0.316	0.0987	59.5
	218.28	67.9	0.312	0.1104	61.0
	217.43	67.2	0.209	0.1199	61.0
	216.97	66.6	0.302	0.1269	61.0
	212.93	62.7	0.268	0.1777	65.2
	207.18	57.6	0.208	0.2410	69.8
	203.01	54.3	0.158	0.2823	72.7
Q ($S-L_1-L_2-V$)	202.32	53.3	0.156	0.2846	73.4
	201.89	51.2	0.183	0.2528	69.9
	201.87	50.9	0.192	0.2423	68.6
	201.82	50.3	0.202	0.2303	67.0
	201.45	48.4	0.239	0.1830	62.9
	201.36	47.9	0.254	0.1717	61.6
	201.23	47.5	0.246	0.1473	60.0
L_1-L_2-V	216.00	65.2	0.289	0.1213	59.8
	216.00	65.0	0.297	0.1087	59.1
	216.00	64.7	0.306	0.0883	58.3
	214.00	62.5	0.292	0.1185	59.7
	214.00	62.2	0.297	0.1006	58.9
	214.00	62.1	0.302	0.0894	57.8
	212.00	61.3	0.260	0.1729	63.6
	212.00	60.9	0.268	0.1619	63.7
	212.00	60.1	0.297	0.1198	58.6
	212.00	59.7	0.288	0.1094	59.7
	212.00	59.7	0.292	0.099	57.7
	210.00	58.5	0.259	0.166	63.2
	210.00	58.1	0.267	0.157	63.1
	210.00	58.0	0.270	0.150	61.6
	210.00	57.4	0.286	0.109	58.4
	208.00	57.0	0.240	0.197	65.2
	208.00	55.9	0.263	0.163	62.1
	208.00	55.4	0.272	0.144	60.6
	208.00	55.5	0.267	0.151	61.8
	206.00	55.9	0.202	0.239	69.4
	206.00	55.2	0.214	0.225	68.7
	206.00	54.3	0.237	0.193	65.0
	206.00	53.5	0.255	0.171	62.5
	206.00	53.0	0.264	0.144	60.4
	206.00	52.9	0.271	0.136	59.6
	204.00	53.7	0.192	0.247	69.5
	204.00	53.6	0.237	0.188	63.9
	204.00	53.2	0.200	0.236	68.6
	204.00	50.5	0.263	0.137	59.7
	202.00	51.3	0.183	0.252	69.9
	202.00	51.0	0.191	0.244	69.2
	202.00	50.5	0.198	0.233	68.2
	202.00	49.1	0.236	0.184	63.6
	202.00	48.4	0.253	0.155	60.8

Grade", with a stated purity of 99.5 mol % and were used without further purification.

The carbon dioxide was "Coleman Grade" (Matheson Co.) with a stated purity of 99.99 mol %. It was prepared by flashing it from the supply cylinder at room temperature into a 3000-mL storage reservoir maintained at 273.15 K. The vapor phase was then vented from the reservoir to remove impurities.

The pressure differences between dew point and bubble point were 0.03 atm at 266.58 K for *n*-butane, 0.41 atm at 298.15 K for carbon dioxide, and 0.10 atm at 286.91 K for propane. The vapor pressure for these three saturated gases at 50 vol % of liquid at these temperatures agreed well with the literature values.

Results

Raw experimental data for the ternary system methane-propane-*n*-octane are presented in Tables I and II. Table

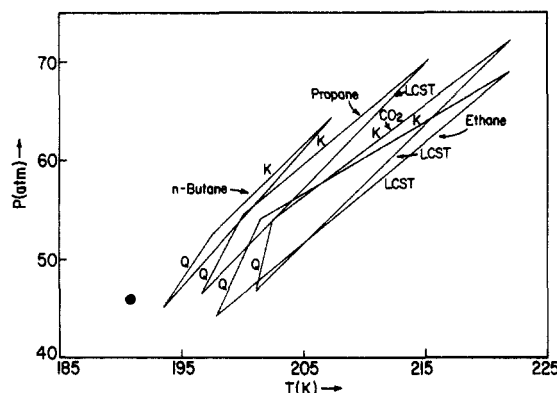


Figure 1. Boundaries of the L_1-L_2-V immiscibility regions of four ternary systems with the common components methane and *n*-octane. The filled circle is the critical point of pure methane.

Table VII. Raw Data of the *n*-Octane-Rich Phase (L_1) for the Binary Carbon Dioxide-*n*-Octane System

type of data			mole fraction of carbon dioxide	mole fraction of <i>n</i> -octane	molar vol, mL/(g mol)
	temp, K	press., atm			
Q ($S-L_1-L_2-V$)	215.99	5.0	0.445	0.5549	101.1
L_1-L_2-V	216.00	5.0	0.444	0.5562	101.5
	217.12	5.3	0.460	0.5401	99.9
	218.00	5.5	0.470	0.5300	99.0
	219.00	5.7	0.491	0.5094	95.9
	220.00	5.9	0.507	0.4934	94.4
	220.79	6.1	0.519	0.4814	93.1
	222.00	6.4	0.527	0.4727	92.9
	225.00	7.2	0.577	0.4226	87.6
	228.00	8.0	0.639	0.3614	80.9
	228.00	8.0	0.639	0.3610	80.5
	229.00	8.3	0.663	0.3374	78.6
	230.00	8.6	0.695	0.3051	74.9
	230.00	8.6	0.692	0.3075	75.0
	230.39	8.7	0.711	0.2888	73.3
	230.48	8.8	0.712	0.2881	72.9
	231.12	9.0	0.749	0.2513	69.1
UCST ($L_1 = L_2-V$)	231.49	9.1	0.802	0.1979	62.8
	231.49	9.1	0.836	0.1644	59.3

I is for the L_2 (*n*-octane-lean) phase while Table II is for the L_1 (*n*-octane-rich) phase. Tables III and IV are for the L_2 and L_1 phases, respectively, of the system methane-*n*-butane-*n*-octane, while Tables V and VI are for the L_2 and L_1 phases, respectively, of the system methane-carbon dioxide-*n*-octane. Included in these tables are raw data on K points, LCST, and Q points which bound the L_1-L_2-V region, in addition to L_1-L_2-V data points. The need for two tables for each ternary system is due to the visual feeling employed in the laboratory, where the data are taken for systems in which phase L_1 is present in an infinitesimal amount (Tables I, III, and V) and for systems in which phase L_2 is present in an infinitesimal amount (Tables II, IV, and VI). The reliability of these data is discussed in the preceding section.

Figure 1 is a pressure-temperature plot of the domains of the three ternary systems studied herein and the domain of the ternary system methane-ethane-*n*-octane studied earlier (1). All four regions are bounded on the high-pressure side by K points, on the low-pressure side by LCST points, and at low temperatures by Q points. The high-temperature limit of each domain appears to be the intersection of the K-point and LCST loci, referred to as the tricritical point. The L_1-L_2-V region has two degrees of freedom according to the phase rule; its boundaries have one.

Tables VII and VIII are raw data for the binary system carbon dioxide-*n*-octane. The three-phase L_1-L_2-V locus is

Table VIII. Raw Data of the *n*-Octane-Lean Phase (L_1) for the Binary Carbon Dioxide-*n*-Octane System

type of data	temp, K	press., atm	mole fraction of carbon dioxide	mole fraction of <i>n</i> -octane	molar vol, mL/(g mol)
			of carbon dioxide	of <i>n</i> -octane	
UCST ($L_1 = L_2-V$)	231.49	0.1	0.836	0.1644	59.3
Q ($S-L_1-L_2-V$)	215.95	5.0	0.978	0.0333	40.3
L_1-L_2-V	217.17	5.2	0.976	0.0242	40.7
	218.85	5.7	0.974	0.0265	41.1
	220.35	6.1	0.971	0.0295	41.9
	221.91	6.4	0.966	0.0336	42.6
	223.96	6.9	0.960	0.0397	43.7
	226.66	7.7	0.947	0.0526	45.5
	231.00	8.9	0.895	0.1046	52.4
	230.00	8.6	0.917	0.0834	49.6
	229.00	8.3	0.939	0.0606	48.0
	228.00	8.0	0.937	0.0628	46.9
	226.00	7.5	0.951	0.0493	45.1

terminated at low temperature by a Q point and at the high-temperature end by a UCST point. Immiscibility occurs in this system at low pressures and is part of a three-phase L_1-L_2-V region unconnected with the one reported in Tables V and VI.

Because the four ternary systems shown in Figure 1 are methane rich, their domains of immiscibility occur near the critical point of pure methane. The binary-solvent critical loci (e.g., that of methane-propane), which evolve out of the methane critical point pass through or close to their respective ternary three-phase immiscibility regions.

Acknowledgment

We are grateful for support of this work provided by the Gas Processors Association (Research Project 795), Tulsa, OK. The research equipment has been built under research grants from the National Science Foundation.

Glossary

C	critical point
K	K point, or critical end point, of an L_1-L_2-V region, where L_2 and V are critical
L_1	liquid phase that is <i>n</i> -octane rich
L_2	liquid phase that is <i>n</i> -octane lean
L_2	liquid phase that is <i>n</i> -octane lean
LCST	lower critical solution point, where L_1 and L_2 are critical
S	solid phase
T	temperature
UCST	same as LCST except it forms an upper terminus to the L_1-L_2-V region
V	vapor phase

Literature Cited

- Hottovy, J. D.; Kohn, J. P.; Luks, K. D. *J. Chem. Eng. Data* 1981, 26, 135.
- Lin, Y.-N.; Chen, R. J. J.; Chappelar, P. J.; Kobayashi, R. *J. Chem. Eng. Data* 1977, 22, 402.
- Kohn, J. P. *AIChE J.* 1981, 7, 514.
- Kohn, J. P.; Bradish, W. F. *J. Chem. Eng. Data* 1984, 9, 5.
- Kohn, J. P.; Kim, Y. J.; Pan, Y. C. *J. Chem. Eng. Data* 1988, 11, 333.
- Rowlinson, J. S. "Liquids and Liquid Mixtures", 2nd ed.; Butterworth: London, 1968; p 214.
- Wagner, J. R.; McCaffrey, D. S.; Kohn, J. P. *J. Chem. Eng. Data* 1988, 13, 22.
- Schnelder, G. *Chem. Eng. Prog. Symp. Ser.* 1968, 64, 9.
- Im, V. K.; Kurata, F. *J. Chem. Eng. Data* 1971, 16, 412.
- Hottovy, J. D.; Luks, K. D.; Kohn, J. P. *J. Chem. Eng. Data* 1981, 26, 258.
- Hule, N. C.; Luks, K. D.; Kohn, J. P. *J. Chem. Eng. Data* 1973, 19, 311.
- Hottovy, J. D. Ph.D. Thesis, University of Notre Dame, Notre Dame, IN, 1980.